JOURNAL OF VIROLOGY, July 1995, p. 4020–4028 Vol. 69, No. 7
0022-538X/95/$04.00+0

Synthesis of Novel Products In Vitro by an RNA-Dependent RNA Polymerase

CHUANZHENG SONG AND ANNE E. SIMON*

Department of Biochemistry and Molecular Biology and Program in Molecular and Cellular Biology, University of Massachusetts at Amherst, Amherst, Massachusetts 01003

Received 12 December 1994/Accepted 20 March 1995

RNA-dependent RNA polymerase from turnip crinkle virus-infected turnip transcribes both strands of a virus-associated satellite RNA, sat-RNA C (356 bases), in vitro. While both plus- and minus-strand sat-RNA C can direct the synthesis of full-length complementary-strand products, transcription of minus-strand RNA also generates two non-template-sized products, L-RNA and S-RNA (C. Song and A. E. Simon, Proc. Natl. Acad. Sci. USA 91:8792–8796, 1994). Here we report that synthesis of L-RNA and S-RNA results from terminal elongation of the 3′ end of the template. L-RNA has a panhandle structure and is composed of minus-strand template covalently linked to newly synthesized RNA complementary to its 5′ 190 bases. S-RNA is composed of template covalently linked to its full-length complementary strand. All minus-strand templates tested yielded S-RNA. However, synthesis of L-RNA was affected by deletion of the 3′ end of the minus-strand template or several internal regions and base alterations near the 5′ end or in an internal sequence immediately upstream from the template-product junction that could potentially form a heteroduplex with the 3′ end. Furthermore, mutations that disrupted or restored a stem-loop involved in RNA recombination in vivo affected the level of L-RNA produced in vitro, suggesting that the mechanisms for intramolecular formation of panhandle RNAs and intermolecular RNA recombination involve similar features.

Positive-strand RNA viruses rely on RNA-dependent RNA polymerases (RdRp) for their replication. RdRp that replicate viral genomes appear to be multisubunit enzymes composed of both virus- and host-encoded polypeptides (3, 13, 30). The absence of proofreading activities during RNA synthesis leads to a nucleotide misincorporation rate of 10^{-3} to 10^{-4} (20, 40). The ability to recombine RNAs by switching templates or jumping within a template during RNA synthesis is also characteristic of many viral RdRp (22, 36). As a result, the evolution rate of RNA viruses is substantially higher than that of the DNA genomes of their hosts.

Partially purified and fully purified RdRp can transcribe cognate RNAs in vitro in either a cyclic manner, producing plus strands from plus-strand templates (3, 17, 42), or a half-cycle synthesis of complementary strands of input plus-strand templates (15, 19, 26, 27, 32, 33). In addition to synthesizing full-length complementary RNAs, several RdRp were able to synthesize products larger than the input templates in vitro. For example, (i) poliovirus RdRp generated dimer-sized (or nearly dimer-sized) RNA transcripts by initiating complementary-strand RNA synthesis through covalent addition of nucleotides to the 3′ end, generated by endonucleolytic cleavage of the template at putative stem-loop structures (18, 25, 43); (ii) partially purified RdRp from cells infected with flock house virus generated dimer-sized transcripts under certain reaction conditions (42); and (iii) RdRp from bacteriophage Qβ synthesized short nucleotide sequences at the 3′ end of the template when initiation was suppressed by replacing GTP with ITP in the reaction mixture (2). It is not known if such 3′-terminal extension is universal among RdRp in vitro reactions or if the sequences and/or structures of the RNA templates play a role in the process.

* Corresponding author. Phone: (413) 545-0170. Fax: (413) 545-4529.

Turnip crinkle virus (TCV) is a monopartite, positive-sense RNA virus consisting of a 4,054-base genomic RNA that encodes five polypeptides (7, 16). TCV is associated with several subviral RNAs, including satellite RNAs (sat-RNAs), which have no sequence homology to the viral genome, and chimeric RNAs, generated through recombination between the genomic and sat-RNAs (38, 44).

RdRp that was partially purified from TCV-infected turnip plants was able to synthesize complementary strands of many TCV-associated subviral RNAs by using minus- or plus-strand templates (39). In addition to template-length products, significant amounts of two products that migrated slower or faster than the full-length form were synthesized from the minus strands of one subviral RNA template under all reaction conditions tested. We now report that the formation of these non-template-length products was due to nucleotide additions to the 3′ end of the template via a copyback mechanism. Furthermore, the 3′ and 5′ ends of the template, an internal guide sequence, and a hairpin structure appear to participate in one copyback event that leads to the production of panhandle-like RNAs.

MATERIALS AND METHODS

RdRp preparation and in vitro transcription. The membrane-containing cell fraction was prepared from leaves of turnip cv. Just Right plants that were infected with TCV genomic RNA, as previously described (39). After detergent treatment, solubilized proteins were separated on a Sephacryl S500HR column (Pharmacia). In vitro transcription was performed with the second of three RdRp activity peaks, which contained little or no endogenous RNA and was specific for exogenously added TCV-associated RNA templates (39). One microgram of RNA template was combined with the RdRp-active fraction, and products were labeled by incorporation of [α-^{32}P]UTP (39) and then analyzed on 42-cm gels containing 5% polyacrylamide and 8 M urea. Nuclease S1 treatment of the radiolabeled products was performed as previously described (39).

Preparation of sat-RNA C templates for in vitro transcription by the RdRp. For preparation of minus-strand templates, oligodeoxynucleotide T7C3′ (5′-GTAATACGACTCACTATAGGGCAGGCCCCCC-3′), which contained a promoter for transcription by T7 RNA polymerase and 13 bases complementary

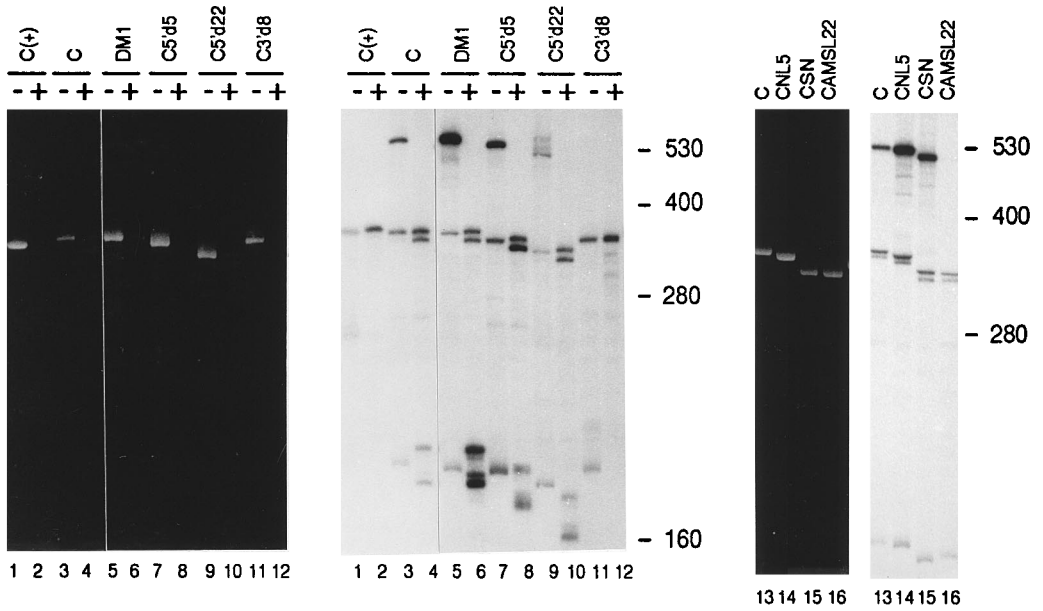

FIG. 1. Denaturing gel analysis of radiolabeled products synthesized by in vitro transcription with RdRp from infected turnip. For lanes 1 through 12, + and − denote products that were treated and not treated with S1 nuclease, respectively. The products shown in lanes 13 to 16 were not treated with S1. Following electrophoresis, gels were stained with ethidium bromide to visualize template RNAs (left panel of each set) and then dried and subjected to autoradiography. The template RNAs, described in Table 1, are indicated above the lanes. All templates were minus-strand orientation except lanes 1 and 2, which were plus-strand sat-RNA C. The positions of RNA markers (in bases) are shown beside the gels. C, minus-strand wild-type sat-RNA C. L-, T-, and S-RNAs generated from the wild-type minus-strand template (lane 3) migrate at positions of 545, 356, and 180 bases, respectively. It is not known why a species migrating slightly faster than template length is synthesized with some RdRp preparations (compare lanes 13 to 16 with lanes 3, 5, 7, 9, and 11).

to the 3′ end of minus-strand sat-RNA C, and C5′ (5′-GGGATAACTAAG GGTTTCA-3′), which is homologous to the 5′ end of minus-strand sat-RNA C, were used to amplify either mutant or wild-type sat-RNA C cDNA by PCR, as previously described (39). For preparation of plus-strand templates, oligodeoxynucleotides T7C5′ (5′-GTAATACGACTCACTATAGGGATAACTAAGG G-3′), which contained the T7 RNA polymerase promoter and 13 bases homologous to the 5′ end of plus-strand sat-RNA C, and C3′ (5′-GGGCAGGCCC CCCGTCCGA-3′), which is complementary to the 3′ end of plus-strand sat-RNA C, were used for the PCR amplification. PCR products were cloned into the *Sma*I site of pUC19. Following *Sma*I digestion of the plasmid, plus- or minus-strand templates containing the exact 3′ and 5′ sequences were synthesized by using T7 RNA polymerase (23). After phenol-chloroform extraction and ethanol precipitation, the RNA concentration was determined by measuring the optical density at 260 nm of the in vitro transcription reaction mix and then subtracting the value contributed by the DNA template. Since the DNA is not a template for the RdRp (39), it was not removed from the DNA-RNA mixture.

Construction of mutant sat-RNA C. CAM, CAMSL22, CAM260, CAM628, CAM182, CAM820, CAMP, CAM456, CAMX, CAM177, and CAM118 were described by Cascone et al. (10). CAMd14 was described by Cascone (8). CSN was described by Simon et al. (37). CNL5 was described by Carpenter et al. (5). pCd3′8 was described by Song and Simon (39). To prepare sat-RNA C cDNA that would generate minus-strand sat-RNA templates with 5′ deletions of 5 or 22 bases or with four altered bases near the 5′ end (DM1), oligodeoxynucleotides that contained the T7 RNA polymerase promoter and sequence homologous to the 5′ end of sat-RNA C, including the deletions or base alterations, were synthesized and used in the PCRs described above. To introduce mutations into the region immediately upstream of the template-product junction, site-directed mutagenesis was performed as described by Kunkel et al. (21) with a partially degenerate oligonucleotide [5′-AACCTGGCT(A/C)(A/G)(A/G)(A/G)GGGA (G/T)TCAAAAGAATCC-3′].

Oligonucleotide-directed RNase H digestions. Radiolabeled L-RNA and S-RNA, synthesized by RdRp in vitro with DM1 and wild-type sat-RNA C templates, respectively, were gel purified and then hybridized to 10 pmol of oligonucleotide in a 9-μl reaction mix containing 4.4 μg of yeast tRNA, 20 mM Tris-HCl (pH 7.5), 10 mM $MgCl_2$, 100 mM KCl, and 0.1 mM dithiothreitol. Control reaction mixes contained equivalent amounts of radiolabeled full-length plus- or minus-strand sat-RNA C transcripts produced by in vitro transcription with T7 RNA polymerase. The reaction mixes were heated at 100°C for 1 min and then slowly cooled to 40°C. One unit of RNase H (Bethesda Research Laboratories [BRL]) was added, and the reaction mixes were incubated at 37°C for 30 min. The products were phenol extracted, precipitated, and then subjected to electrophoresis on 42-cm 7% polyacrylamide–8 M urea gels. The oligonucleotides complementary to plus-strand sat-RNA C sequence were C3′, 3′-terminal 19 bases; 1, positions 12 to 36; and 13, positions 250 to 269. Oligonucleotides homologous to plus-strand sat-RNA C (for detection of minus strands) were C5′, 5′-terminal 19 bases; 22, positions 115 to 132; and DM4, positions 206 to 223. The numbering of sat-RNA C is according to Simon and Howell (38).

Cloning the L-RNA template-product junction. L-RNA was synthesized with the DM1 template, gel purified, and then hybridized to oligonucleotide 22 (homologous to positions 115 to 132 of sat-RNA C) followed by digestion with RNase H. The radioactive product was purified and then subjected to reverse transcription (RT)-PCR amplification (6). RT was performed with oligonucleotide C3′ (complementary to the 3′-terminal 19 bases) and Moloney murine leukemia virus reverse transcriptase (BRL). Oligonucleotides 3, which is complementary to positions 99 to 113 of sat-RNA C, and C3′ were used for PCR. The ~290-bp PCR fragment was gel purified, cloned into the *Sma*I site of pUC19, and then sequenced.

RACE PCR. One microgram of gel-purified minus-strand sat-RNA C transcripts synthesized by T7 RNA polymerase or of gel-purified L-RNA or S-RNA synthesized by RdRp transcription was polyadenylated with yeast poly(A) polymerase (US Biochemicals) under the conditions recommended by the manufacturer. Amplification of the 3′-end sequences of minus-strand sat-RNA C transcripts synthesized by T7 RNA polymerase was done by the RACE protocol (14), with oligonucleotide 3 as the sat-RNA C-specific oligonucleotide.

RESULTS

In vitro transcription with minus-strand templates results in formation of products that migrate faster and slower than the full-length form. In vitro transcription of plus-strand sat-RNA C (356 bases) with RdRp isolated from TCV-infected plants resulted in the synthesis of one major product that migrated to the position of full-length complementary RNA (Fig. 1, lanes 1 and 2). Minus-strand sat-RNA C, however, directed the synthesis of three major products, as revealed by polyacrylamide-urea gel electrophoresis: template-length RNA (T-RNA), larger-than-template-length RNA (L-RNA), and smaller-than-template-length RNA (S-RNA) (Fig. 1, lane 3).

The minus strands of sat-RNA C containing a variety of previously generated deletions were transcribed by the RdRp for initial characterization of the L- and S-RNA products (Fig.

TABLE 1. Effect of mutations on synthesis of L-RNA

Template	Mutation(s)	Relative L-RNA/T-RNA ratio[a]	Recombination[b]	Infectivity[c]
C	None	1.00	Y	Y
CAM	U-209→G	1.11 ± 0.12	Y	Y
CAM628	U-184→G, A-201→C	0.83 ± 0.19	Y	Y
CAM820	U-182→G, A-205→C	0.24 ± 0.06	Y	Y
CAMX	G-170→U, U-171→C	0.46 ± 0.14	Y	Y
CAM79	C-175→U	2.76 ± 0.17	Y	Y
CAM177	U-177→G	0.63 ± 0.02	Y	Y
CAMSL22	Δ57–78	0.10 ± 0.05	Y	N
CAM182	U-182→G	0.07 ± 0.04	N	Y
CAM260	U-184→G	0.17 ± 0.05	N	Y
CAMP	G-194→A, U-195→C	0.13 ± 0.04	N	Y
CAM118	A-188→U	0.62 ± 0.03	N	Y
CAMd14	Δ148–161	0.12 ± 0.07	N	Y
CmHTR	166-GGGAAAC-160→166-CCCUCCU-160	0.12 ± 0.01	NT	NT
DM1	353-CAGG-349→AUAA	5.30 ± 1.84	NT	NT
CSN	Δ79–100	2.20 ± 0.73	NT	Y
CNL5	Δ96–100	2.18 ± 0.62	NT	Y
C3′d8	Δ1–8	0.06 ± 0.04	NT	NT
C5′d5	Δ352–356	1.32 ± 0.08	NT	NT
C5′d22	Δ335–356	2.33 ± 0.34	NT	NT

[a] Levels of L-RNA were determined by densitometer scanning of autoradiograms for two to three independent experiments and are expressed as the ratio of L-RNA to T-RNA. Standard deviations are given. The ratio of L-RNA to T-RNA for wild-type minus-strand sat-RNA C was normalized to 1.00, and the ratios for the mutants are expressed as a fraction of the wild-type ratio. The L-RNA/T-RNA value for wild-type C(−) was 1.38 ± 0.26 (seven independent experiments).

[b] The ability to recombine with sat-RNA D was assayed by Cascone et al. (10). Y, yes; N, no; NT, not tested.

[c] The infectivity of the plus-strand RNAs of mutant constructs was described previously (see Materials and Methods for references).

1 and Table 1). Deletion of 5 bases from the 5′ end of the minus-strand sat-RNA C template had no effect on the levels of L-RNA, S-RNA, or T-RNA (Fig. 1, lane 7), while deletion of 22 bases at the 5′ end decreased the overall transcription efficiency of the template without affecting the ratio of the three RNAs (Fig. 1, lane 9). Deletion of 8 bases from the 3′ end eliminated the formation of L-RNA without affecting the synthesis of T-RNA or S-RNA (Fig. 1, lane 11), indicating a requirement for specific 3′-end sequences in the generation of L-RNA. Deletion of 22 bases in the 3′ region (positions 57 to 78; all numbering is from the corresponding plus strand) resulted in a substantial reduction in the level of L-RNA and a slight reduction in the level of T-RNA (Fig. 1, lane 16; low levels of L-RNA were visible in overexposed autoradiograms); transcripts containing this deletion are not infectious in vivo (10). Additional nearby deletions of 22 or 5 bases (positions 79 to 100 and 96 to 100, respectively) resulted in an increase of about twofold in the level of L-RNA without affecting T-RNA or S-RNA levels (Fig. 1, lanes 14 and 15). In vivo, plants inoculated with plus-strand RNA containing these deletions (along with TCV helper virus) accumulated substantially higher levels of dimeric sat-RNA C than the wild type (4, 5, 37).

To test the effect that base-pairing between the 3′ and 5′ ends might have on synthesis of L-RNA, four bases were altered near the 5′ end of the minus strand (5′-GGGCAGGC to 5′-GGGAUAAC; mutant DM1), which would allow eight paired residues with the 3′ end (3′-CCCUAUUG). Transcription of the DM1 template resulted in an approximately fivefold increase in the amount of L-RNA synthesized while slightly decreasing the levels of T-RNA (Fig. 1, lane 5).

After S1 nuclease digestion, transcripts migrating to the positions of L-RNA and S-RNA were not detected. Rather, three new S1-resistant RNAs were visible on denaturing gels (Fig. 1, lanes 4, 6, 8, and 10). The high level of the S1-resistant doublet bands migrating near the 180-base position with RNA synthesized from DM1 mutant transcripts (Fig. 1, lane 6) and the absence of the doublet bands with C3′d8, which lacked the L-RNA product (Fig. 1, lane 12), suggested that the doublets were double-stranded segments of L-RNA. As described below, the S1-resistant species that migrated slightly faster than the T-RNA was derived from S1 treatment of S-RNA (see Fig. 6). However, it is not known why this S1-resistant species is not found for C3′d8 (8-base deletion at the 3′ end; lane 12).

L-RNA is generated by 3′-terminal elongation of the template molecules. When products synthesized in vitro with the wild-type minus-strand sat-RNA C template were subjected to lengthy electrophoresis through 42-cm polyacrylamide-urea gels, L-RNA migrated at a position corresponding to 545 bases. L-RNAs produced with a template containing the 5′-terminal 22-base deletion (C5′d22) or the internal deletion of positions 79 to 100 (CSN) were reduced in size by about 44 and 22 bases, respectively (data not shown). This suggested that the 5′ end of sat-RNA C was present twice in the L-RNA, while this internal 22-base region was present only once.

From these data, two models were proposed for the formation of L-RNA (Fig. 2). In the internal-initiation model, the RdRp initiates transcription at or near a stem-loop that is the crossover site for the generation of recombinant RNAs between sat-RNA C and another satellite RNA (sat-RNA D [10]). After internal initiation near the stem-loop, L-RNA could be generated by the RdRp's transcribing to the 5′ end of the template and then reinitiating synthesis at the 3′ end without releasing the nascent RNA; interaction between the two ends of the templates might be important in mediating the reinitiation of transcription at the 3′ end (Fig. 2A). This internal initiation mechanism would produce an RNA containing one full-length plus strand (356 bases) joined to about 185 bases of 3′-terminal plus-strand sequence.

A second possible mechanism is terminal elongation, resulting in the formation of a panhandle-like RNA (Fig. 2B); the RdRp elongates the 3′ end of the template by synthesizing a sequence complementary to the 5′-terminal region, initiating from a site at or near where recombination occurs. The result-

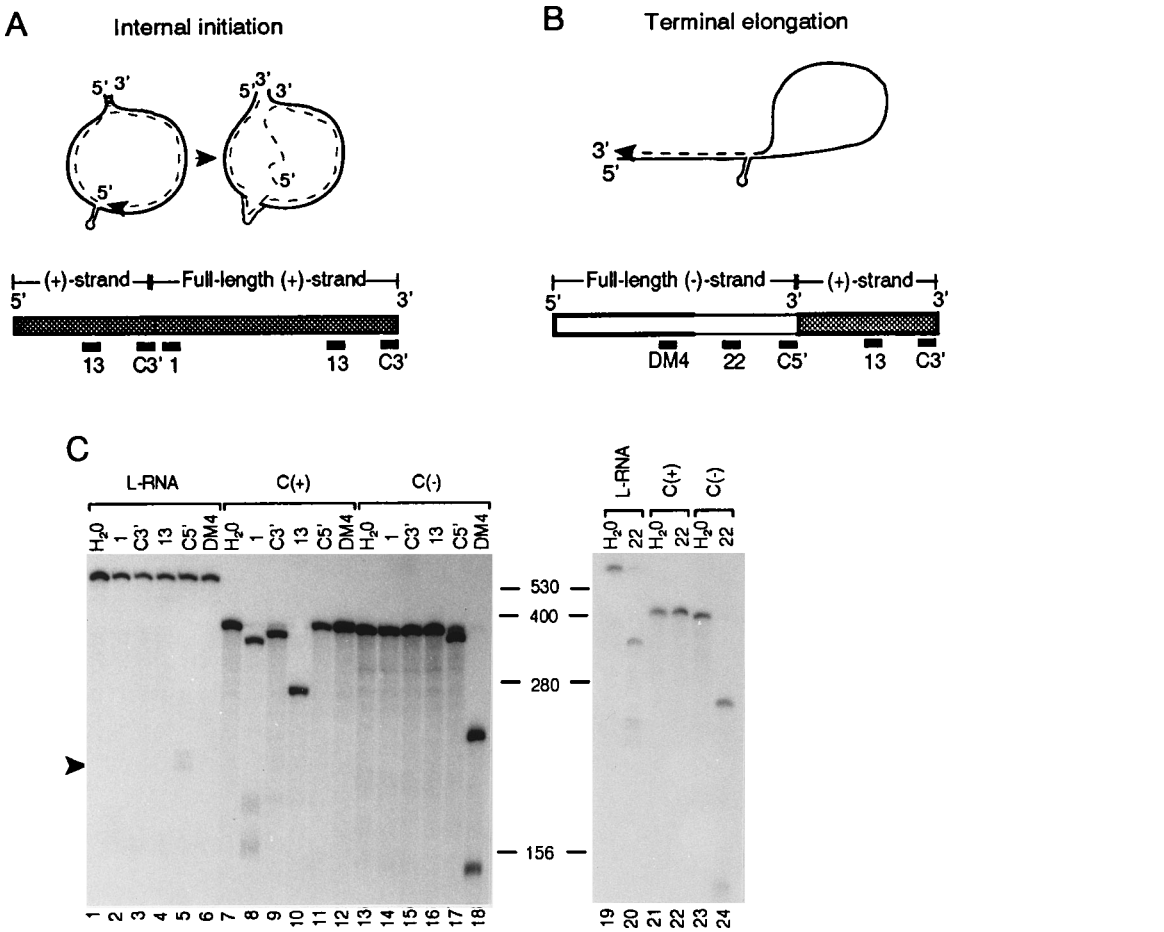

FIG. 2. Possible mechanisms of L-RNA formation. (A) Internal-initiation model. (B) Terminal-elongation model. Template and nascent RNAs are denoted by solid and dashed lines, respectively. The products produced by such mechanisms are diagrammed below each model. Minus-strand template and nascent plus-strand RNAs are represented by open and shaded boxes, respectively. The two base-paired regions in the product produced by terminal elongation are denoted by thick lines. The solid bars indicate the positions of oligonucleotides used for RNase H digestion. (C) Denaturing gel analysis of RNase H-digested ^{32}P-labeled L-RNA and sat-RNA C full-length plus- and minus-strand T7 RNA polymerase-synthesized transcripts. Purified RNAs were hybridized to the oligonucleotides denoted above each lane (or H_2O) prior to RNase H treatment. The position of the low-level L-RNA digestion product (lane 5) with oligonucleotide C5′ is indicated by an arrowhead. The positions of RNA markers (in bases) are shown beside the gels.

ant species would consist of full-length minus-strand template and about 190 bases of newly synthesized plus-strand sequence complementary to the 5′ portion of the minus-strand template. The L-RNA would therefore contain approximately 185 bp of double-stranded sequence and 175 bases of single-stranded, minus-strand sequence.

To distinguish between these two models, ^{32}P-labeled L-RNA was generated by RdRp-mediated in vitro transcription with minus-strand DM1 as the template (which produced about fivefold more L-RNA than the wild-type template). Gel-purified L-RNA was hybridized to oligonucleotides complementary to either the minus or plus strand of sat-RNA C and then digested with RNase H (Fig. 2C). Three oligonucleotides which hybridized to the plus-strand sat-RNA C sequence and promoted the digestion of full-length plus-strand transcripts (C3′, 1, and 13) did not lead to digestion of the L-RNA (Fig. 2C, lanes 2 to 4). This suggested that the L-RNA was not generated by the internal initiation mechanism proposed in Fig. 2A. One oligonucleotide (DM4) which hybridized to the minus-strand sequence within the putative double-stranded region of L-RNA produced by template-elongation (Fig. 2B) also did not promote digestion with RNase H (Fig. 2C, lane 6). This lack of cleavage was likely due to the unavailability of the target sequence (see below). L-RNA hybridized to oligonucleotides with sequences complementary to the putative single-stranded sequence of template-elongated L-RNA (C5′ and 22) was either partially or completely digested following treatment with RNase H (Fig. 2C, lanes 5 and 20). The sizes of the radiolabeled fragments following digestion were consistent with L-RNA being produced by terminal elongation at an internal sequence. Incomplete digestion of the L-RNA with the C5′ oligonucleotide may have resulted from the target site's being sterically only partially available for probe binding or RNase H digestion, because of the proximity of the complementary sequences to the double-stranded region (see below).

These results suggest that L-RNA is a panhandle-like RNA composed of both template and newly synthesized sequences. To determine if L-RNA is synthesized in an intramolecular reaction, as shown in Fig. 2B, or a bimolecular reaction, whereby the 3′-end extension occurs from a second template molecule, minus-strand sat-RNA C transcripts containing either an 8-base deletion at the 3′ end (C3′d8) or a deletion of positions 148 to 161 (CAMd14) were subjected together to in

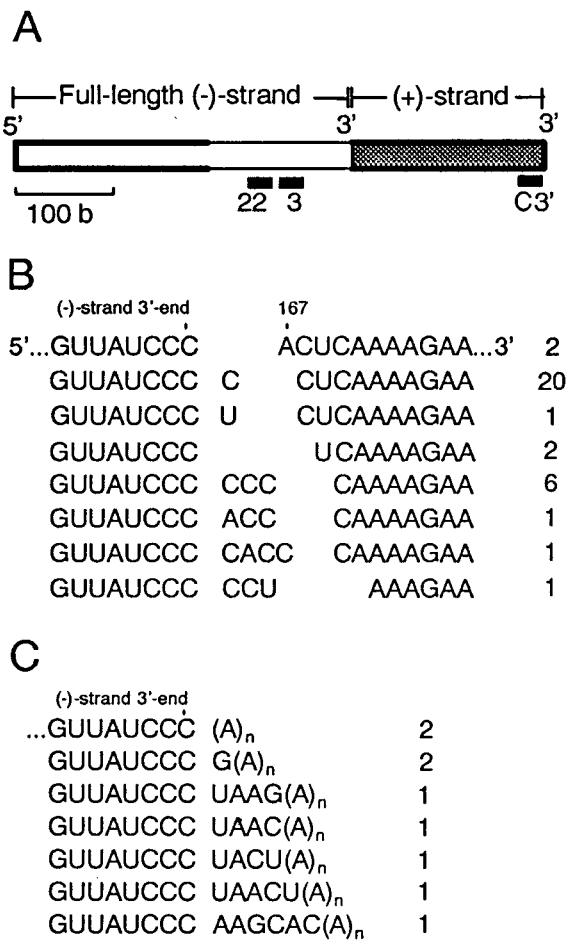

FIG. 3. Cloning and sequencing of the L-RNA template-product junction. (A) Diagram of L-RNA (see legend to Fig. 2 for explanation) and the oligonucleotides used for the PCR cloning. The two complementary segments (represented by the thick lines) were separated by RNase H digestion of L-RNA hybridized to oligonucleotide 22. Oligonucleotides 3 and C3′ were then used in RT-PCR amplification of the RNA fragment containing the template-product junction. (B) Sequence of the template-product junction. Numbers to the right represent the number of clones with the junction sequences indicated. Nontemplate nucleotides at the junction separate the 3′ end of the template (left) and the nascent plus-strand sequences (right). The nascent sequence begins around position 167 of plus-strand sat-RNA C (42). (C) The 3′-terminal sequences of minus-strand sat-RNA C transcripts generated by in vitro transcription with T7 RNA polymerase. Transcript RNA was polyadenylated and then subjected to RACE PCR, cloning, and sequencing. The numbers of clones with each type of sequences are shown to the right.

vitro transcription with RdRp from TCV-infected plants. Although neither of these transcripts alone yielded L-RNA (Fig. 1, lane 11; also see Fig. 4, lane 3), the occurrence of a bimolecular reaction could allow the normal 3′ end of CAMd14 to extend on the normal internal region of C3′d8. No additional L-RNA was synthesized in reaction mixes containing the two templates, however, suggesting that the formation of L-RNA is an intramolecular reaction (data not shown).

Cloning and sequencing of the template-product junction. L-RNA generated from DM1 RNA transcripts was gel purified and subjected to full-length amplification by RACE PCR (14). cDNA products, however, were not generated by this procedure, possibly because of the putative terminal base-pairing between the 5′ and 3′ ends. To separate the 5′ and 3′ ends, gel-purified L-RNA was hybridized with oligonucleotide 22 (Fig. 3A), which is complementary to a sequence in the putative single-stranded region, and then digested with RNase H. The single radioactive fragment (~310 bases) was purified and subjected to RT-PCR amplification with primers complementary to the 3′-terminal 19 bases (oligonucleotide C3′) and positions 99 to 113 of plus-strand sat-RNA C (oligonucleotide 3) (Fig. 3A). PCR amplification produced cDNA of ~290 bp, the size expected if the L-RNA was generated by template elongation, as proposed in Fig. 2B (data not shown).

Sequencing of 34 L-RNA cDNA clones confirmed that the 3′ end of the minus-strand template was joined to the nascent plus-strand sat-RNA C sequence (Fig. 3B). The L-RNA species was found to comprise a population of RNA molecules with slightly different template-product junctions. All clones contained junctions between the 3′ end of the minus-strand template and positions 167 to 172 of the nascent plus strand. Thirty clones (88%) also contained between one and four nontemplate nucleotides at the junction position, most commonly a single C residue. No other differences were found in the cDNAs. Dimers of sat-RNA C, hypothesized to be generated by a recombination event, frequently have either a single U residue or between one and five additional C residues at the junctions (4, 38); these nontemplate residues are similar to the extra bases found at the L-RNA junctions. Terminal nontemplate nucleotide incorporation activity has also been found for the RdRp of Qβ bacteriophage (1), peanut stunt virus (11), and cucumber mosaic virus (12) and from uninfected tomato leaves (34).

T7 RNA polymerase has also been reported to add one or two nontemplate nucleotides to the 3′ ends of RNA transcripts during in vitro transcription (28). Since the minus-strand sat-RNA C templates were produced by in vitro transcription with T7 RNA polymerase, it was necessary to determine the composition of any nontemplate bases already present on the sat-RNA C transcripts. The 3′ ends of gel-purified minus-strand transcripts were polyadenylated with poly(A) polymerase and then amplified by RACE PCR (14). As shown in Fig. 3C, seven of nine cDNA clones contained between one and six random, nontemplate bases at the 3′ ends of the transcripts. This was surprising, since only one or two bases were added to transcripts synthesized in the previous study (28), although these transcripts were much smaller (12 to 24 bases) than sat-RNA C. The non-template bases that were found on the 3′ end of the minus-strand sat-RNA C transcripts were more random than the extra bases at the junctions in the L-RNA, suggesting that the TCV replicase was responsible for the additional residues. However, it is also possible that L-RNA is generated by selective elongation of only certain species in the population of minus-strand sat-RNA C templates.

Sequence and/or structure near the internal extension site is important for L-RNA synthesis. Comparison of sequences in minus-strand sat-RNA C located 3′ to position 167 and at the 3′ end indicated possible base-pairing between the terminal and internal sequences that might potentiate the 3′-end extension (Fig. 4A). As a preliminary test of this possibility, the sequence from positions 160 to 166 was altered from GG GAAAC to CCCUCCU, which would disrupt the putative heteroduplex between the 3′ end and the internal region. The mutant template (CmHTR) was subjected to in vitro transcription with RdRp isolated from TCV-infected turnip. The results indicated a decrease of more than eightfold in the amount of L-RNA synthesized with the mutant template compared with the wild-type template (Fig. 4B, lane 2, and Table 1; L-RNA was visible in overexposed autoradiograms). In addition, deletion of 14 bases (positions 148 to 161) in the sequence possibly involved in the heteroduplex (CAMd14) decreased the level of L-RNA by a similar amount (Fig. 4B, lane 3, and Table 1).

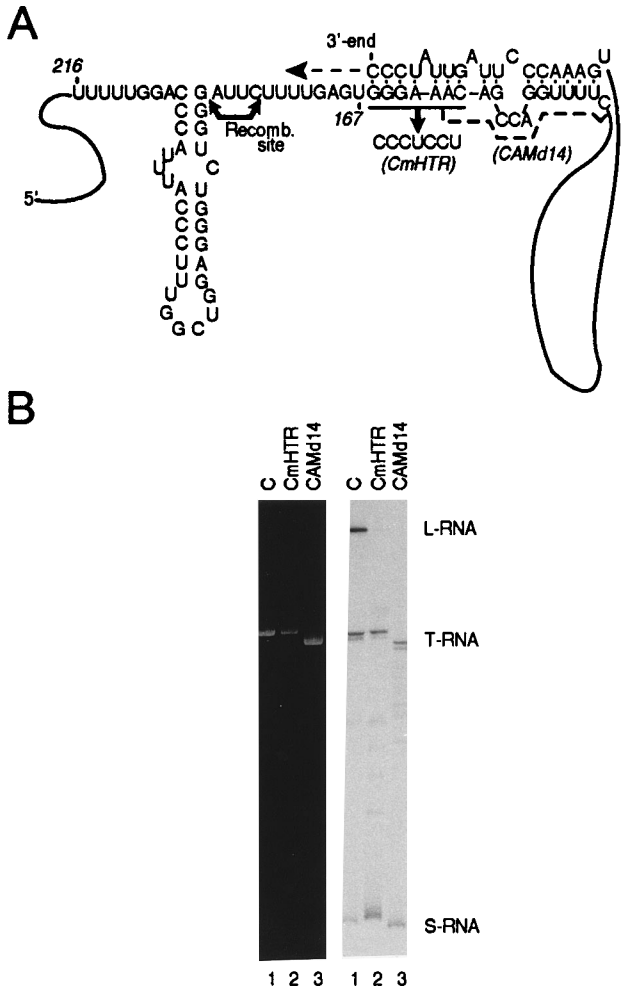

FIG. 4. Effect of mutations 3′ to the template-product junction on the synthesis of L-RNA. (A) Potential base-pairing between the 3′ end and the region immediately upstream from the template-product junction (approx. position 167). The positions of base changes in CmHTR and the deletion (dashed line below sequence) in CAMd14 are indicated. (B) Denaturing gel analysis of ^{32}P-labeled products synthesized from the templates indicated above the lanes. The ethidium bromide-stained gel is shown to the right of the corresponding autoradiogram. The positions of L-RNA, T-RNA, and S-RNA are indicated.

Since low levels of L-RNA were still synthesized with CmHTR and CAMd14, putative priming of the 3′ end on the internal sequence by base-pairing may facilitate the terminal elongation event but is not absolutely required.

Located only 12 bases 5′ to position 167 is a stem-loop structure (motif I hairpin [10]) that is involved in the generation of recombinant molecules between sat-RNAs D and C in vivo (9, 10). The recombination crossover site is located at the base of the motif I hairpin (positions 174 to 178). Based in part on the sequence similarity between downstream recombination junctions in a variety of TCV-associated recombinant molecules and the 5′ ends of viral genomic, subgenomic, and subviral RNAs, recombination is thought to occur during plus-strand synthesis: the RdRp dissociates from the minus-strand sat-RNA D template without releasing the nascent RNA and reinitiates synthesis at one of the crossover sites at the base of the motif I hairpin. The motif I hairpin structure might therefore be an internal RdRp recognition signal that directs the template switch by the TCV RdRp in vivo. It is plausible that the same signal may also contribute to the in vitro generation of L-RNA, which, like RNA recombination, involves 3′-terminal elongation. To test this postulation, minus-strand RNAs derived from a variety of constructs previously used to assess the effect of point mutations in the motif I hairpin region on recombination in vivo were assayed for their ability to generate L-RNA (Fig. 5A and Table 1). The levels of L-RNA synthesized are presented as a ratio of L-RNA to T-RNA in Table 1 to normalize for possible discrepancies in sample loading, to compare between different experiments, and to account for mutations that affect overall template efficiency and not L-RNA synthesis specifically. As can be seen from Fig. 5B, the level of T-RNA (and S-RNA) did not vary substantially among the wild type and mutants; therefore, the ratio of L-RNA to T-RNA obtained with these mutant templates is an approximation of the increase or decrease in L-RNA levels compared with the wild type.

Four of five alterations previously found to eliminate detectable recombinants reduced the amount of L-RNA synthesized to between 7 and 17% of the wild-type level without substantially affecting the synthesis of T-RNA or S-RNA (CAM182, CAM260, CAMP, and CAMd14; Fig. 5B, lanes 3, 5, and 7; Fig. 4B, lane 3). Two of these mutants (CAM260 and CAM182) involved single base alterations in the stem of the hairpin (U to G at positions 184 and 182, respectively), predicted by computer secondary-structure analysis to markedly alter the structure of the region (10). Compensatory changes, designed to "correct" for the mutations in CAM260 and CAM182 by conversion from wild-type UA to GC in the hairpin stem (CAM628 and CAM820; see Fig. 5A), restored RNA recombination (10) and produced L-RNA levels that were 4.9- or 3.4-fold higher than the L-RNA levels found for the single mutations (Fig. 5B, lanes 4 and 6). In addition, all mutations near the recombination crossover site that were previously found to permit the accumulation of recombinants in planta produced high levels of L-RNA in vitro, between 46 and 276% of the wild-type level (CAM, CAM177, CAM79, and CAMX).

Although our results suggest a correlation between the ability to recombine and the ability to synthesize large amounts of L-RNA, there were two exceptions that should be noted. CAM118, which contains an A to U alteration at position 189 in the hairpin stem, generated 62% of the wild-type level of L-RNA, similar to several of the mutations that did not affect recombination (Fig. 5B, lane 8). The computer algorithm predicted a substantially altered hairpin structure for RNA containing this mutation, and no recombinants were detected in vivo. Furthermore, deletion of bases 57 to 78 (CAMSL22), which resulted in noninfectious transcripts (10), substantially reduced the level of L-RNA while allowing recombination (see Fig. 1, lane 16). This deletion, however, was nearly 100 bases upstream of the recombination crossover site and may have had an effect on L-RNA synthesis that was unrelated to sequence and structural requirements for recombination.

S-RNA is also produced by 3′-terminal extension of the minus-strand sat-RNA C template. In vitro transcription of the minus-strand sat-RNA C template with isolated RdRp also produced a major product (S-RNA) that migrated at the 180-base position on polyacrylamide-urea gels. The inability to amplify S-RNA by RACE PCR and to digest gel-purified S-RNA with RNase H and any plus- or minus-strand-specific oligonucleotides suggested that S-RNA was not a single-stranded product generated by internal initiation and/or premature termination (data not shown). When gel-purified S-RNA was subjected to S1 nuclease digestion, two bands that migrated near the position of full-length complementary strands were generated (Fig. 6, compare lanes 2 and 3). These

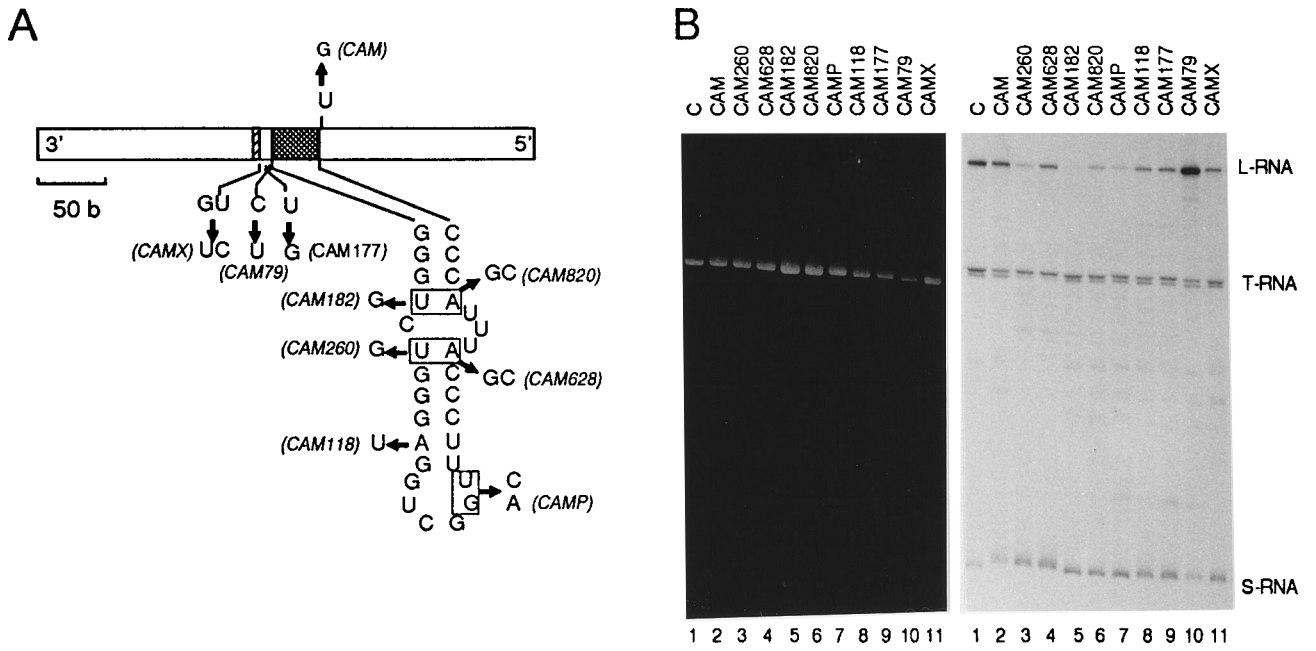

FIG. 5. Effect of mutations 5′ to the template-product junction on L-RNA synthesis. (A) Locations of mutations in minus-strand sat-RNA C. All mutants also contained the U to G CAM mutation. The shaded region marks the position of the hairpin near the recombination crossover site. The hatched region marks the position of the template-product junction in L-RNA. (B) Denaturing gel analysis of RNAs synthesized by RdRp from TCV-infected turnip in vitro. All templates were of the minus-strand orientation. The gel was stained with ethidium bromide (left), dried, and exposed to X-ray film to visualize the ^{32}P-labeled products. The positions of L-RNA, T-RNA, and S-RNA are indicated.

results suggest that S-RNA is a double-stranded hairpin RNA, with the nascent strand covalently bound to the 3′ end of the template. This product therefore resembles the dimer-sized transcripts produced by poliovirus RdRp (43).

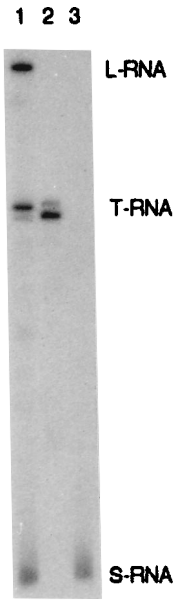

FIG. 6. Characterization of S-RNA. Radiolabeled S-RNA synthesized from the minus-strand sat-RNA C template was gel purified and subjected to S1 nuclease treatment. Lane 1, total products synthesized from the minus-strand sat-RNA C template; lane 2, gel-purified S-RNA treated with S1 nuclease; lane 3, untreated gel-purified S-RNA. The positions of untreated L-RNA, T-RNA, and S-RNA are indicated.

DISCUSSION

We have identified two non-template-length RNAs generated by in vitro transcription of minus-strand sat-RNA C with partially purified TCV RdRp: the hairpin-like S-RNA, composed of template covalently linked to its complementary strand, and panhandle-like L-RNA, composed of template and covalently linked newly synthesized RNA complementary to the 5′ 190 bases of the minus-strand sat-RNA C template.

Hairpin-like products that migrated much faster than T-RNA on acrylamide-urea gels were generated for all mutant RNAs subjected to in vitro transcription with the RdRp (39, 39a; this report). Synthesis of RNAs with panhandle-like characteristics only occurred when minus-strand templates with wild-type 3′ ends or with a deletion of 114 3′-terminal bases were used (39). This suggests that, unlike synthesis of S-RNA, synthesis of L-RNA has specific 3′-end sequence requirements. In addition, deletions and base alterations in several regions of sat-RNA minus strands affected the synthesis of L-RNA but not S-RNA. Deletion of positions 148 to 161 (CAMd14) or alteration of bases 160 to 166 (CmHTR) led to greatly decreased levels of L-RNA, which could have resulted from disruption of putative base-pairing with the 3′-end sequence. Deletion of bases 57 to 78 also abolished L-RNA synthesis, possibly because of altered secondary structure affecting the 3′ end and/or internal regions.

If a duplex between the 3′ end and sequences at positions 143 to 166 facilitates the priming of 3′-terminal extension, then it is unclear why altering four nucleotides near the 5′ end (DM1) induced higher levels of L-RNA synthesis (see Fig. 1, lane 5). Furthermore, the 5′ end is not required for L-RNA synthesis; deletion of five bases at the 5′ end had no effect on L-RNA levels, while deletion of 22 bases reduced the level of all products (see Fig. 1, lanes 7 and 9). One possible explanation is that there are several different structural conformations

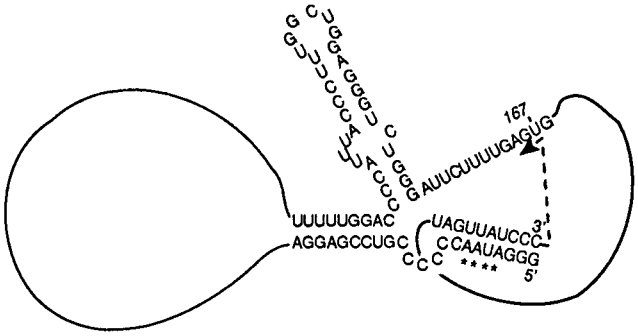

FIG. 7. Model for enhancement of L-RNA synthesis with transcripts (DM1) containing four base alterations near the 5′ end (denoted by asterisks) designed to promote base-pairing with the 3′ end. The model suggests that base-pairing between the 3′ and 5′ ends together with base-pairing between sequences near the 5′ end and directly 5′ of the hairpin shown in Fig. 4A helps to position the 3′ end near the internal site where terminal elongation takes place. The dashed line marks the position of the 3′-end extension on the internal template sequence.

that can lead to 3′-terminal extension: one promoted by heteroduplex formation at positions 143 to 166, and the second involving interaction between the 3′ and 5′ ends. Interestingly, a structure can be formed in which base-pairing between the 3′ and 5′ ends, and between sequences near the 5′ end and downstream from the recombination stem-loop, may aid in positioning the 3′ end near the internal extension template (Fig. 7).

Sequence and structural elements near the crossover site in sat-RNA C where recombination occurs with sat-RNA D appear to influence the synthesis of L-RNA. Mutations that disrupted the stem or loop (with the exception of CAM118) of a hairpin required for recombination decreased the level of L-RNA, while compensatory mutations that reformed the stem-loop structure increased the level of L-RNA synthesized over levels produced by the single mutations. One compensatory change (U-182 to G and A-205 to C [CAM820]), however, resulted in only 24% of wild-type L-RNA levels. This suggests that sequence as well as structural requirements in the region can influence the synthesis of L-RNA. From our results with recombination among TCV-associated RNAs, we believe that this stem-loop, which includes a sequence similar to the 5′ end of TCV genomic RNA and other recombination junctions, may serve as an RdRp internal recognition signal. For synthesis of L-RNA, the RdRp may interact with the stem-loop and elongate from the 3′-end hydroxyl group of the nearby heteroduplex. Alternatively, disruption of the stem-loop may perturb the structure of the region involved in heteroduplex formation with the 3′ end.

It is possible that L-RNA and S-RNA are only produced under artificial in vitro conditions and not in TCV-infected plants. L-RNA was not infectious when inoculated with TCV genomic RNA onto turnip plants (data not shown), suggesting that even if present in infected cells, L-RNA is likely a nonproductive product of viral RNA replication. Hairpin RNAs derived from the viral genomic RNA, however, have been detected in cells infected with poliovirus (31, 43), and defective interfering RNAs with hairpin and panhandle structures have been found in cells infected with two negative-strand RNA viruses, vesicular stomatitis virus and Sendai virus (35). In the former case, the hairpin RNAs are believed to be dead-end RNA products generated by terminal elongation after nicking at stem-loop structures on the template (31). In the latter case, the panhandle-like defective interfering RNAs may play a role in modulating the balance between transcription and replication (41).

Since 3′-terminal extension of RNA on an RNA template occurs during RNA-RNA recombination, and since mutations that affect the synthesis of L-RNA also affect RNA recombination, it is possible that some examples of RNA recombination that cannot be explained by the processive heteroduplex-mediated model of brome mosaic virus (29) may occur by nonprocessive extension of primers. In this terminal-elongation mechanism, the 3′-end sequences of a "priming" RNA forms a limited heteroduplex with a template RNA near an RdRp recognition structure or sequence; after binding to this heteroduplex recognition signal complex, the RdRp elongates from the 3′-end hydroxyl group of the priming RNA, forming a recombinant RNA composed of the original priming RNA and newly synthesized RNA complementary to the template RNA. Some recombinant molecules associated with TCV (6, 6a) and flock house virus (24) have short regions of base-pairing at crossover sites at a frequency higher than expected for a purely random occurrence. However, for both TCV and flock house virus, numerous recombinants that would have mismatched terminal nucleotides are formed, indicating that pairing of the terminal nucleotide is not a requirement for recombination. The acquisition of cellular RNA by RNA viruses (22) could also have occurred by primer extension, with tRNAs or RNA fragments generated by RNA degradation providing a source of primers for RNA recombination.

ACKNOWLEDGMENTS

We thank Clifford Carpenter for critical reading of the manuscript.

This work was supported by National Science Foundation grants MCB 9315948 and MCB-9419303 to A.E.S. and by a University of Massachusetts graduate fellowship to C.S.

REFERENCES

1. **Bausch, J. N., F. R. Kramer, E. A. Miele, C. Dobkin, and D. R. Mills.** 1983. Terminal adenylation in the synthesis of RNA by Qβ replicase. J. Biol. Chem. **258:**1978–1984.
2. **Biebricher, C. K., and R. Luce.** 1992. *In vitro* recombination and terminal elongation of RNA by Qβ replicase. EMBO J. **11:**5129–5135.
3. **Blumenthal, T., and G. G. Carmichael.** 1979. RNA replication: function and structure of Qβ replicase. Annu. Rev. Biochem. **48:**525–548.
4. **Carpenter, C. D., P. J. Cascone, and A. E. Simon.** 1991. Formation of multimers of linear satellite RNAs. Virology **183:**586–594.
5. **Carpenter, C. D., P. J. Cascone, and A. E. Simon.** 1991. Mutations in a satellite RNA of turnip crinkle virus result in addition of poly(U) *in vivo*. Virology **183:**595–601.
6. **Carpenter, C. D., and A. E. Simon.** 1994. Recombination between plus and minus strands of turnip crinkle virus. Virology **201:**419–423.

6a. **Carpenter, C. D., and A. E. Simon.** Unpublished data.

7. **Carrington, J. C., L. A. Heaton, D. Zuidema, B. I. Hillman, and T. J. Morris.** 1989. The genome structure of turnip crinkle virus. Virology **170:**219–226.
8. **Cascone, P. J.** 1992. Ph.D. dissertation, University of Massachusetts, Amherst.
9. **Cascone, P. J., C. D. Carpenter, X. H. Li, and A. E. Simon.** 1990. Recombination between satellites of turnip crinkle virus. EMBO J. **9:**1709–1715.
10. **Cascone, P. J., T. F. Haydar, and A. E. Simon.** 1993. Sequences and structures required for recombination between virus-associated RNAs. Science **260:**801–805.
11. **Collmer, C. W., A. Hadidi, and J. M. Kaper.** 1985. Nucleotide sequence of the satellite of peanut stunt virus reveals structural homologies with viroid and certain nuclear and mitochondrial introns. Proc. Natl. Acad. Sci. USA **82:**3110–3114.
12. **Collmer, C. W., and J. M. Kaper.** 1985. Double-stranded RNAs of cucumber mosaic virus and its satellite contain an unpaired terminal guanosine: implication in replication. Virology **145:**249–259.
13. **David, C., R. Gargouri-Bouzid, and A.-L. Haenni.** 1992. RNA replication of plant viruses containing an RNA genome. Prog. Nucleic Acid Res. Mol. Biol. **42:**157–227.
14. **Frohman, M. A., M. K. Dush, and G. R. Martin.** 1988. Rapid production of full-length cDNAs from rare transcripts: amplification using a single gene-specific oligonucleotide primer. Proc. Natl. Acad. Sci. USA **85:**8998–9002.
15. **Gargouri-Bouzid, R., C. David, and A.-L. Haenni.** 1991. The 3′ promoter

region involved in RNA synthesis directed by the turnip yellow mosaic virus genome in vitro. FEBS Lett. **294:**56–58.
16. **Hacker, D. L., I. T. D. Petty, N. Wei, and T. J. Morris.** 1992. Turnip crinkle virus genes required for RNA replication and virus movement. Virology **186:**1–8.
17. **Hayes, R. J., and K. W. Buck.** 1990. Complete replication of a eukaryotic virus RNA in vitro by a purified RNA-dependent RNA polymerase. Cell **63:**363–368.
18. **Hey, T. D., O. C. Richards, and E. Ehrenfeld.** 1987. Host factor-induced modification during synthesis of poliovirus RNA in vitro. J. Virol. **61:**802–811.
19. **Houwing, C. J., and E. M. J. Jaspars.** 1986. Coat protein blocks the in vitro transcription of viron RNAs of alfalfa mosaic virus. FEBS. Lett. **209:**284–288.
20. **Kearney, C. M., J. Donson, G. E. Jones, and W. O. Dawson.** 1993. Low level of genetic drift in foreign sequences replicating in an RNA virus in plants. Virology **192:**11–17.
21. **Kunkel, T. A.** 1985. Rapid and efficient site-specific mutagenesis without phenotypic selection. Proc. Natl. Acad. Sci. USA **82:**488–492.
22. **Lai, M. M. C.** 1992. RNA recombination in animal and plant viruses. Microbiol. Rev. **56:**61–79.
23. **Li, X. H., and A. E. Simon.** 1991. In vivo accumulation of a turnip crinkle virus defective interfering RNA is affected by alterations in size and sequence. J. Virol. **65:**4582–4590.
24. **Li, Y., and L. A. Ball.** 1993. Nonhomologous RNA recombination during negative-strand synthesis of flock house virus RNA. J. Virol. **67:**3854–3860.
25. **Lubinski, J. M., G. Kaplan, V. R. Racaniello, and A. Dasgupta.** 1986. Mechanism of in vitro synthesis of covalently linked dimeric RNA molecules by the poliovirus replicase. J. Virol. **58:**459–467.
26. **Miller, W. A., and T. C. Hall.** 1983. Use of micrococcal nuclease in the purification of highly template-dependent RNA-dependent RNA polymerase from brome mosaic virus-infected barley. Virology **125:**236–241.
27. **Miller, W. A., and T. C. Hall.** 1984. RNA-dependent RNA polymerase isolated from cowpea chlorotic mottle virus-infected cowpeas is specific for bromoviral RNA. Virology **132:**53–60.
28. **Milligan, J. F., D. R. Groebe, G. W. Witherell, and O. C. Uhlenbeck.** 1987. Oligoribonucleotide synthesis using T7 RNA polymerase and synthetic DNA templates. Nucleic Acids Res. **15:**8783–8798.
29. **Nagy, P. D., and J. J. Bujarski.** 1993. Targeting the site of RNA-RNA recombination in brome mosaic virus with antisense sequences. Proc. Natl. Acad. Sci. USA **90:**6390–6394.
30. **Quadt, R., C. C. Kao, K. S. Browning, R. P. Hershberger, and P. Ahlquist.** 1993. Characterization of a host protein associated with brome mosaic virus RNA-dependent RNA polymerase. Proc. Natl. Acad. Sci. USA **90:**1498–1502.
31. **Richards, O. C., T. D. Hey, and E. Ehrenfeld.** 1987. Poliovirus snapback double-stranded RNA isolated from infected HeLa cells is deficient in poly(A). J. Virol. **61:**2307–2310.
32. **Sanker, S., and A. G. Porter.** 1991. Expression, purification, and properties of recombinant encephalomyocarditis virus RNA-dependent RNA polymerase. J. Virol. **65:**2993–3000.
33. **Saunder, K., and P. Kaesberg.** 1985. Template-dependent RNA polymerase from black beetle virus-infected *Drosophila melanogaster* cells. Virology **144:**373–381.
34. **Schiebel, W., B. Haas, S. Marinkovic, A. Klanner, and H. L. Sanger.** 1993. RNA-directed RNA polymerase from tomato leaves. II. Catalytic in vitro properties. J. Biol. Chem. **263:**11858–11867.
35. **Schlesinger, S.** 1988. The generation and amplification of defective interfering RNAs, p. 167–185. *In* E. Domingo, J. J. Holland, and P. Ahlquist (ed.), RNA genetics. CRC Press, Boca Raton, Fla.
36. **Simon, A. E., and J. J. Bujarski.** 1994. RNA-RNA recombination and evolution in virus-infected plants. Annu. Rev. Phytopathol. **32:**337–362.
37. **Simon, A. E., H. Engel, R. P. Johnson, and S. H. Howell.** 1988. Identification of regions affecting virulence, RNA processing and infectivity in the virulent satellite of turnip crinkle virus. EMBO J. **7:**2645–2651.
38. **Simon, A. E., and S. H. Howell.** 1986. The virulent satellite RNA of turnip crinkle virus has a major domain homologous to the 3′ end of the helper virus genome. EMBO J. **5:**3423–3428.
39. **Song, C., and A. E. Simon.** 1994. RNA-dependent RNA polymerase from plants infected with turnip crinkle virus can transcribe (+)- and (−)-strands of virus-associated RNAs. Proc. Natl. Acad. Sci. USA **91:**8792–8796.
39a. **Song, C., and A. E. Simon.** Unpublished data.
40. **Ward, C. D., M. A. Stoke, and J. B. Flanegan.** 1988. Direct measurement of the poliovirus polymerase error frequency in vitro. J. Virol. **62:**558–562.
41. **Wertz, G. W., S. Whelan, A. LeGrone, and L. A. Ball.** 1994. Extent of terminal complementarity modulates the balance between transcription and replication of vesicular stomatitis virus RNA. Proc. Natl. Acad. Sci. USA **91:**8587–8591.
42. **Wu, S. X., P. Ahlquist, and P. Kaesberg.** 1992. Active complete in vitro replication of nodavirus RNA requires glycerophospholipid. Proc. Natl. Acad. Sci. USA **89:**11136–11140.
43. **Young, D. C., D. M. Tuschall, and J. B. Flanegan.** 1985. Poliovirus RNA-dependent RNA polymerase and host cell protein synthesize product RNA twice the size of the poliovirion RNA in vitro. J. Virol. **54:**256–264.
44. **Zhang, C., P. J. Cascone, and A. E. Simon.** 1991. Recombination between satellite and genomic RNAs of turnip crinkle virus. Virology **184:**791–794.